Organic & Biomolecular Chemistry

Accepted Manuscript

ROYAL SOCIETY OF CHEMISTRY

www.rsc.org/obc

Cite this: DOI: 10.1039/c0xx00000x

www.rsc.org/xxxxxx

ARTICLE TYPE

Disodium cromoglycate: exploiting its properties as a NMR weak-aligning medium for small organic molecules

Eduardo Troche-Pesqueira,[a] María Magdalena Cid*[a] and Armando Navarro-Vázquez*[a]

Received (in XXX, XXX) Xth XXXXXXXXX 20XX, Accepted Xth XXXXXXXXX 20XX

DOI: 10.1039/b000000x

Chromonic phases are a family of lyotropic liquid crystals (LC) formed by ionic aromatic mesogens as disodium cromoglycate (cromolyn), sunset yellow and others. It is well known that chromonic phases are oriented in the presence of external magnetic fields, leading to the observation of anisotropic NMR observables such as quadrupolar splittings or residual dipolar couplings. Despite the fact that the cromolyn nematic LC phase (N) presents important advantages like great homogeneity, small line broadening, and easy sample preparation, it has been scarcely used as a water-compatible NMR orienting medium, in part due to a too strong induced degree of alignment on the guest molecules. However, the use of cromolyn/brine mixtures led to optimum degree of alignment allowing to record ^{1}H-^{13}C dipolar couplings with good accuracy.

Introduction

Structural elucidation of small organic molecules in solution assisted by NMR in weak-aligned media has been greatly developed in the last years mainly due to the development of organic solvent compatible weak-aligning media,[1,2] which allow observation of residual dipolar couplings (RDCs) with a magnitude comparable to *J* couplings. Developments in pulse sequences[3,4,5,6] and software analysis[7] have also contributed to the advances in the field. RDCs have been successfully applied to the configurational analysis of complex molecules, even in complex molecules with a high degree of conformational flexibility.[8,9]

Depending on the solvent, degree of alignment required and other factors, a number of alignment media for the structural determination of small organic molecules have been reported in the past years, mainly lyotropic liquid crystals[10,11,12,13] and stretched cross-linked polymers.[14,15,16,17,18] Lyotropic phases are the *go to* option in the case of water-soluble molecules, where only polyacrylamide polymers[19] are an alternative to them. When it comes to dealing with molecules soluble in organic solvents, polypeptide (PBLG, PELG) based liquid crystals comprise an alternative to cross-linked polymers.

A family of lyotropic LCs not yet sufficiently explored regarding their NMR properties are the so-called chromonic phases.[20,21,22,23] They were mainly investigated by Lydon and co-workers although in the last years they have attracted attention of many research groups, and a wealth of applications have been developed for this kind of compounds, such as compensators,[24] biosensors[25,26,27] or polarizers.[28] Chromonic phases are formed by aggregation of small ionic aromatic mesogens in water and are named after disodium cromoglycate (DSCG), an antiasthmatic drug known by the commercial names of Cromolyn and INHALT (**Fig. 1**). As a general fact, chromonics are rigid aromatic planks in opposition to soap-like LCs, which tend to be large flexible aliphatic rods. The molecules are supposed to self-aggregate in columns in a face-to-face fashion,[29] giving place majorly to two types of phases: the nematic phase (N), composed of individual columnar domains, and the hexagonal phase (M) at higher concentrations, with a regular two-dimensional lattice.[20]

DSCG is known to be oriented in the presence of a magnetic field.[30] However its use as a NMR alignment medium has not been very widespread, and only Cortieu and co-workers have used it in order to differentiate between *R* and *S* 1-deutero-1-phenylethanol using β-cyclodextrin as chiral auxiliary.[31]

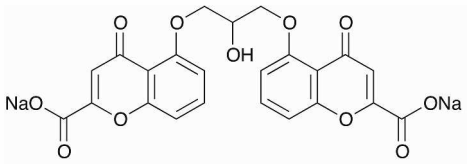

Fig. 1 Disodium cromoglycate (cromolyn).

In this work, we want to explore the scope and limitation of DSCG as a weak-aligning phase for practical applications in structural elucidation of small molecules. We will determine suitable mesogen concentration ranges as well as the influence of addition of brine since it is known that its addition modifies the phase diagram of DSCG.[32] From here we will call the brine-doped phase N^{d}. Since one of the main issues of aligning phases can be inhomogeneity throughout the sample, we will investigate the spatial distribution of the degree of alignment of DSCG LC phases using recently developed deuterium NMR imaging techniques.[33]

DSCG behaviour has been tested on a variety of samples regarding their polarity and structural complexity, going from small rigid molecules without conformational flexibility and few ^{1}H–^{13}C vectors, to more complicated ones, with larger conformational spaces and several chiral centres (**Fig. 2**). We used as probes two saccharides, a water-soluble non-ionic polycyclic alcohol, and a water-soluble quaternary ammonium iodide alkaloid derivative.

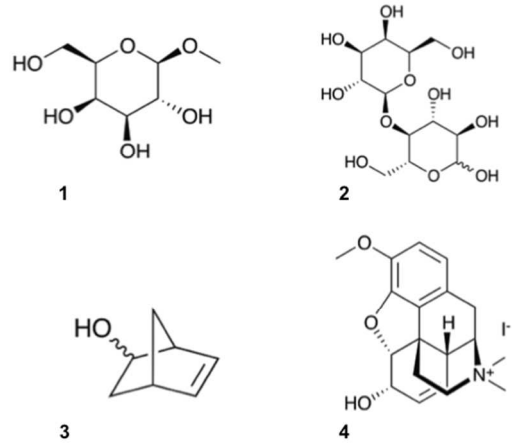

Fig. 2 Molecules used to test DSCG as alignment medium: 1) methyl-β-D-galactopyranoside, 2) D-(+)-lactose, 3) 5-norbornen-2-ol, 4) *N*-methyl-codeinium iodide.

Results and discussion

^{1}H and ^{2}H NMR studies

DSCG's phase diagram was the first one recorded and published among the different chromonic phases,[34,35] showing a characteristic multi-peritectic form. The phase diagram shows that at 25ºC the nematic (N) phase is formed from 12 wt% of DSCG in water up to 18 wt%. Between 18 and 21 wt% both nematic (N) and hexagonal (M) phases co-exist, and beyond that point the phase is completely hexagonal.

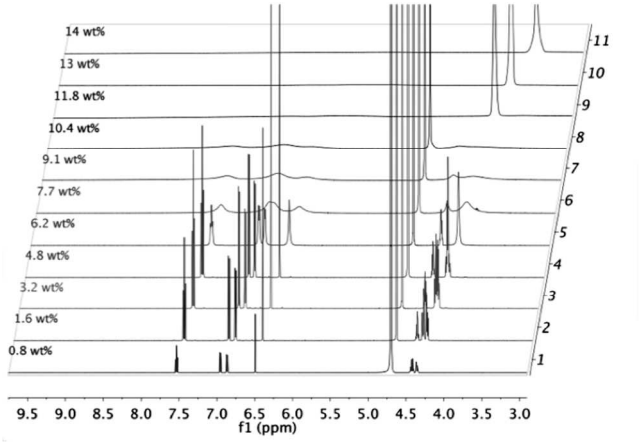

Fig. 3 ^{1}H DSCG spectra in D_2O at different concentrations, from dilute solutions, up to concentrations where the nematic phase should be formed according to its phase diagram.

By performing ^{1}H and ^{2}H experiments in the regions where the isotropic, isotropic+nematic, nematic, nematic+hexagonal and hexagonal phases were expected to be found, we were able to determine which one would be more suitable for performing RDC NMR experiments. As a result of the self-aggregation process, the lines in the ^{1}H NMR spectra get broader as the concentration of DSCG increases, up to a point (7.7 wt%) when aliphatic ^{1}H signals completely overlap and the multiplicity is lost (**Fig. 3.6**). This phenomenon becomes dramatic beyond 11.8 wt% concentration (**Fig. 3.9**), when the liquid crystal starts to form, according to its phase diagram. Beyond this point, line broadening increases in such a way that ^{1}H signals are no longer observable. The formation of the liquid crystal carries with it two phenomena responsible for the increment in the line broadening, i.e. sample aggregation, which shortens T_2 relaxation times, therefore broadening lines, and the arousal of dipolar couplings between the nuclei of the monomer unit. The combination of these phenomena makes DSCG signals so broad that they not interfere with the molecules studied using it as alignment medium. The effect of liquid crystal phase formation on line-broadening of DSCG signals can be clearly observed in a comparison between two ^{1}H spectra of DSCG at the same concentration (7.7 wt%), one in D_2O (**Fig. 4a**) where only aggregation is occurring yet, and in a brine doped phase (**Fig. 4b**), which allows the formation of the LC phase at that concentration, making DSCG proton signals to completely vanish.

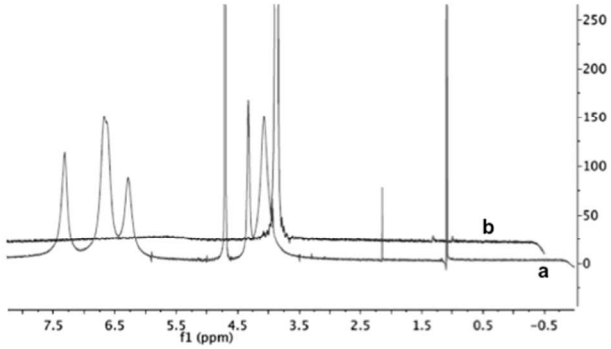

Fig. 4 Comparison of the ^{1}H spectra of DSCG at 7.7 wt% in a) D_2O and b) in the sample doped with brine (0.3 M).

In an alignment medium, inspection of the deuterium splitting ($|\Delta\nu_Q|$), which arises from the deuterium quadrupole interaction with its spin in an anisotropic environment, is one of the routine methods to determine the degree of alignment. The phase transition was confirmed by the ^{2}H spectrum, since the singlet observed in the isotropic phase splits into a doublet, as can be seen in **Fig. 5**. At concentrations where the hexagonal phase has been reported to form, the deuterium splitting is larger (498 Hz at 25 wt% of DSCG in D_2O) than in the nematic phase, and the peaks become asymmetric and broad (**Fig. 6**).

It is known that doping aqueous solutions with different salts can either stabilize or disrupt the formation of this type of liquid crystals depending on the size of the cation.[20,32] In our case, the addition of brine allows the DSCG molecules to self-aggregate at lower concentrations (between 7.7 and 11.8 wt%), also showing a smaller $|\Delta\nu_Q|$ (85 Hz at 7.7 wt%), more suitable for NMR experiments in alignment media, and sharper peaks. However, at DSCG concentrations where the nematic phase is formed already without the help of brine, its addition seems to not have consequences on the ordering of the phase, and at 14 wt% of cromolyn in D_2O, the deuterium splitting barely differs in magnitude from the N to the N^d phase (**Fig. 5**).

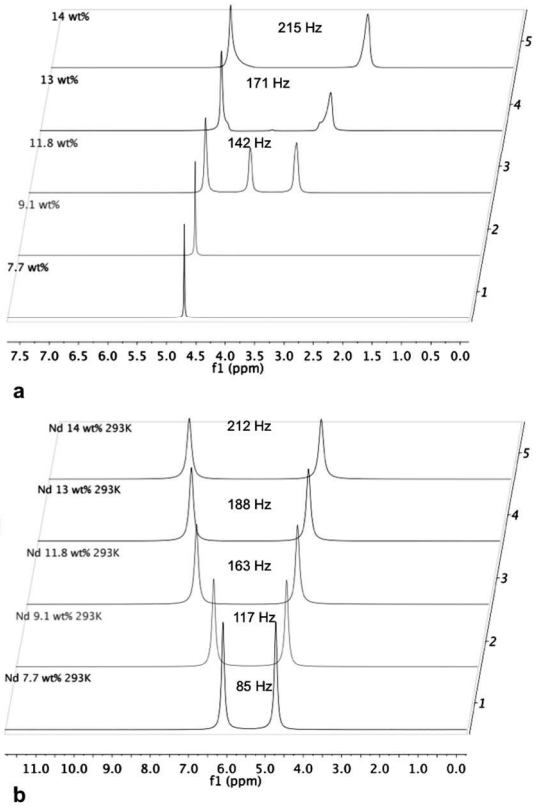

Fig. 5 Comparison between the DSCG N and the N^d phases ^2H $|\Delta_Q|$splittings at different concentrations at 293K.

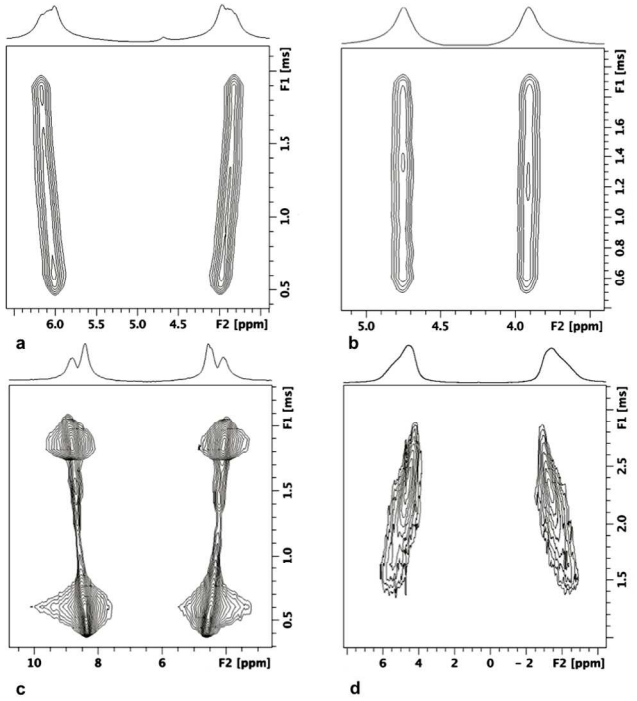

Fig. 6 2D ^2H images of a) 14 wt% DSCG nematic phase (N), b) 7 wt% DSCG nematic phase doped with brine (N^d), c) 21 wt% DSCG hexagonal phase (M) and d) 25 wt% DSCG hexagonal phase (M). Note that TopSpin labels by default the *y* axis in ms instead of mm. It can be seen in the experimental section how to perform the unit conversion.

Deuterium imaging

As shown in previous work by Gil and co-workers,[33] acquisition of 1D ^2H spectra does not suffice to unravel magnetic field and sample inhomogeneities along the *z* direction of anisotropic samples, since these properties are space-averaged. Therefore, spatial resolved NMR can be used to divide the sample into slices, acquire individual spectra of each one and build up an image in a pseudo-2D fashion, making use of pulsed field gradients (PFGs) technology. A sequence that uses a selective excitation pulse in the presence of a gradient was used to perform the experiments. The homogeneity of the regular nematic phase (**Fig. 6a**), of the nematic phase formed by doping the DSCG with brine (**Fig. 6b**) and the hexagonal phase (**Fig. 6c** and **d**) at different concentrations, was checked.

It can be observed that both nematic phases show great homogeneity along the *z* direction of the sample. Concentration gradients are not observed and only a smaller alignment degree in the bottom of the sample can be seen in the regular nematic phase (N). This would account for some line broadening in the 1D ^2H spectrum, which has yet similar values for both phases (8.10 Hz for the N *vs* 8.01 Hz for the N^d phase). On the other hand, both M phase samples show large concentration gradients in the bottom and top of the sample and different alignment degrees along the *z* direction of the samples. This physical inhomogeneity in the hexagonal samples is responsible for the large increment in the line broadening of the doublet peaks and for the asymmetry they show.

Temperature phase-dependency

Phase transitions in lyotropic LC are also sensitive to temperature changes, which is very important for sample preparation. By heating the LC phases, they can turn completely isotropic, allowing to transfer them easily to the NMR tubes. The temperatures needed for samples to become isotropic in the N and N^d phase are very mild, as can be seen in **Fig. 7** (308 and 302K respectively). On the other hand, samples at the hexagonal phase concentration ranges (>21 wt%), need to be heated up to 80ºC, which makes sample preparation quite difficult. This fact, along with the poor homogeneity of the phase observed in the 2D ^2H experiments, led us to not monitor phase transition changes in the hexagonal phase by NMR. Also, temperature plays a crucial role in the protocol we decided to use to perform the shimming in our samples. When doing NMR experiments in lyotropic LC, shimming is one of the main issues for having a good spectral resolution and signal to noise ratio and manual shimming becomes cumbersome when the LC phase is formed. Hence, we decided to heat up the samples to the point where they become isotropic, perform an automatic shimming routine, and then let the sample cool down slowly and equilibrate until the anisotropic phase is fully recovered. By doing this, we assume an error, since shimming parameters are also temperature dependants. Because of equipment conveniences, most of our RDC related experiments were performed at 293K. Therefore, being able to perform shimming at the closest temperature to 293K would reduce this error, allowing the record of high quality NMR spectra.

By acquiring ^2H spectra at different temperatures, the change from anisotropic/nematic to isotropic phase was monitored in

both N and N^d phases. Inspection of 1D ^{2}H spectra for these two samples showed that by doping the nematic phase with brine, not only the nematic phase is stabilized, but also the difference between the shimming temperature and the one we choose to perform our experiments, is shorter than in the N phase (9 *vs* 15ºC respectively). A really interesting fact is that the ability of this samples to turn back and forth into either isotropic or anisotropic conditions, would allow to acquire the RDC related experiments of the sample under study in both experimental conditions just by raising the temperature a few degrees Celsius, with minor differences in the values extracted with respect to the ones extracted in D_2O (

Table 1), as will be shown later. Also, the region where both isotropic and nematic phases co-exist is very interesting, since *a priori*, it could allow to have both sets of signals (isotropic and anisotropic) in the same experiment. In order to test this hypothesis, HSQC ^{1}H–^{13}C and HETCOR ^{13}C–^{1}H coupled experiments were conducted in the N^d phase at 299K and indeed, isotropic and anisotropic signals were observed (see Supporting Information). However, the difference in ^{1}H or ^{13}C chemical shifts of the cross-peaks was not enough to allow simultaneous recording of ^{1}H-^{13}C couplings in both phases. All these features encourage the use of the N^d phase, mainly due to the smaller degree of alignment it imparts and superior sample homogeneity.

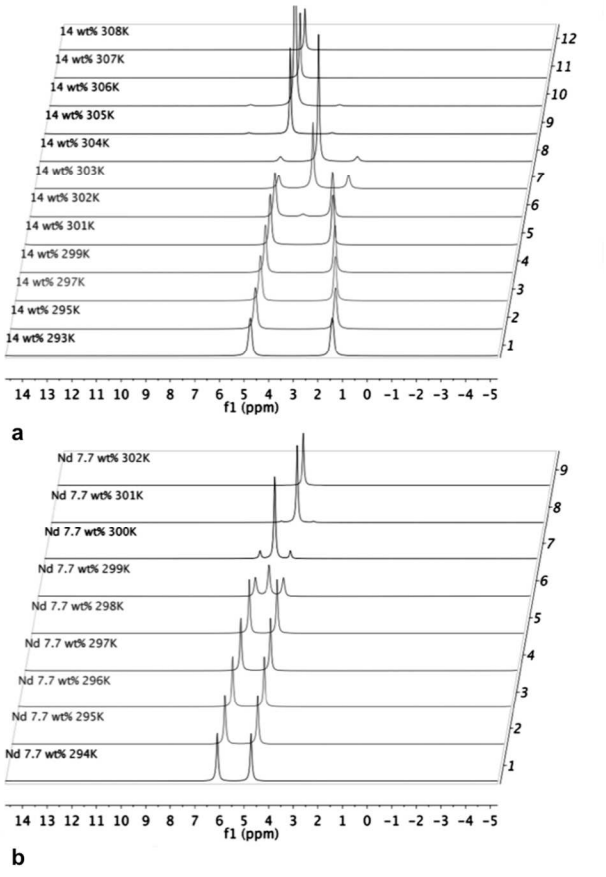

Fig. 7 ^{2}H spectra of DSCG samples at a) 14 wt% in D_2O and b) 7 wt% in D_2O/NaCl at different temperatures.

Methyl-β-D-galactopyranoside and D-(+)-lactose

As first probe to test the alignment properties of DSCG phases on a "guest" molecule, we chose a monosaccharide like methyl-β-D-galactopyranoside (**Fig. 2.1**) with few independent ^{1}H-^{13}C vectors and a small conformational space. In such a simple molecule, ^{13}C gated-decoupled experiment sufficed to measure $^1J_{CH}$ and $^1T_{CH}$ couplings in isotropic and anisotropic conditions respectively (**Fig. 8**). RDCs for each ^{1}H-^{13}C pair were calculated subtracting the scalar coupling to the total ($^1D_{CH}$=$^1T_{CH}$-$^1J_{CH}$). Three experiments were performed in anisotropic conditions: in the 14 wt% DSCG N phase (**Fig. 8b**), in the 7 wt% DSCG N^d phase (**Fig. 8c**) and in the 25 wt% DSCG M phase (**Fig. 8d**). RDC data extraction was not possible for all the ^{1}H-^{13}C pairs in the experiment in the hexagonal phase, since line broadening was too large, causing signals to overlap in the region of carbon atoms C2, C3, C4 and C5. Also the baseline was worse than in the other experiments even after applying a baseline correction, and the S/N ratio was smaller. On the other hand, it was feasible to extract $^1T_{CH}$ from the N and N^d phases. However the latest showed better peak resolution (**Fig. 8b**), and $^1D_{CH}$ RDC values extracted from this experiment had a more manageable magnitude (3-33 Hz in N^d *vs* 10-99 Hz in N).

Methyl-β-D-galactopyranoside samples were also used to check if the degree of alignment and magnitude of the residual dipolar couplings show or not any dependency with the magnetic field. F2-coupled HSQC experiments were performed at two different NMR frequencies, 400 and 600 MHz in both N and N^d phases. The differences in the extracted total couplings are within the error in the measurement (see Supporting Information) and therefore it can be concluded that they are not dependent on the frequency at which the NMR works. The ^{2}H quadrupolar splittings for the N phase kept a constant value of 200 Hz in going from 400 to 600 MHz spectrometers whereas for the N^d phase the splitting slightly increased from 85 to 89 Hz.

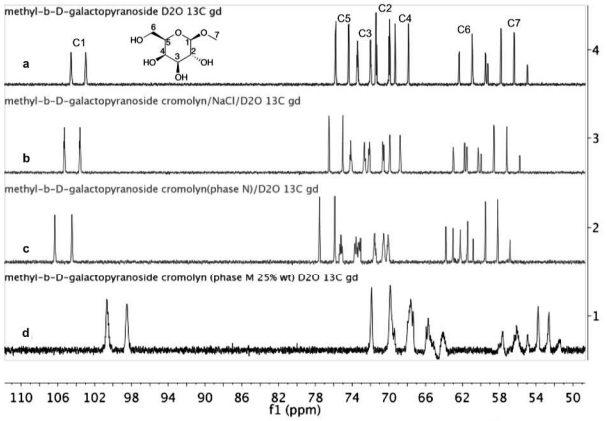

Fig. 8 Stacked ^{13}C gated decoupled methyl-β-D-galactopyranoside spectra a) in isotropic conditions (D_2O), b) in the 7.7 wt% N^d phase, c) in the 14 wt% N phase and d) in the 25 wt% DSCG/D_2O hexagonal phase.

In going to more structurally complex molecules, the use of the ^{13}C gated decoupled experiment is no longer possible due to signal overlapping and instead we employed a BIRD-filtered *J*-scaled F1-coupled HSQC[5,36,37] where the combination of a *J*-evolution multiplication factor (κ) with a BIRD-filter in order to supress long-range couplings allows to downscale the error in the extraction of the $^1J_{CH}$ and $^1T_{CH}$ couplings without extending the experimental time.[38] When dealing with methylene groups in F1

coupled experiments, only the outer lines of their triplets (or doublet of doublets) are observed, being the separation between these lines equal to the sum of the two individual couplings. This makes that the only data available for methylene groups would be the average of the sum of the coupling of each methylene carbon with its two protons. This can be a problem in small systems with few independent ^{1}H-^{13}C vectors, but in most it has the advantage that diastereotopic methylene protons do not need to be assigned and extraction of the sum of the coupling in the ABX spin system is much less affected by strong couplings. These methylene couplings can be then directly incorporated in the RDC fitting using the MSpin program.[39,40] Therefore, the rest of the molecules tested in this work were studied using this experiment.

A sample of D-(+)-lactose (**Fig. 2b**) in which both α and β anomers for the glucose moiety were present in solution in a ratio 38/62 in favour of the β anomer, which is kept constant in the anisotropic phase, was used as the next probe molecule. Signal assignment was done with a combination of COSY and HSQC correlations. A set of 18 RDCs was extracted, 6 for the galactose ring, 6 for α-glucose and 6 for β-glucose. Also, vicinal $^{3}D_{HH}$ couplings for the anomeric protons were extracted using just the 1D ^{1}H spectrum for the scalar couplings and Mueller's P.E.COSY experiment[41] for the total couplings. β-Lactose structures from a molecular dynamics run were DFT optimized and RDC data sets were fitted to the resultant pool of structures. The results were evaluated in terms of the Cornilescu quality factor (Q)[42] and the SVD[43] condition number (both implemented in the software MSpin[7]), which is used as a measure of how well conditioned a system is, i.e. large condition numbers usually indicate a lack of enough vectors to determine a system. A quality factor of 0.068 and a SVD condition number of 7.8 were obtained for β-lactose assuming the syn-syn conformation as the only significantly present in solution.[44] Besides the expected discrimination between anomers, the results obtained showed again that great quality data is obtained using the brine doped DSCG LC phase with really good resolution and relatively short acquisition times.

Table 1 D-(+)-Lactose a) $^{1}J_{CH}$ and $^{3}J_{HH}$ couplings in isotropic conditions in D_2O and b) in the nematic doped phase (N^d) at 303K, c) $^{1}T_{CH}$ and $^{3}T_{HH}$ couplings in the N^d phase at 293K, and d) and e) $^{1}D_{CH}$ and $^{3}D_{HH}$ couplings calculated as $D=T-J$ for each $^{1}J_{CH}$ and $^{3}J_{HH}$ data set (see D-(+)-lactose assignment in SI).

Atom	$^{1}J_{CH}$ (Hz)[a]	$^{1}J_{CH}$ N^d (Hz)[b]	$^{1}T_{CH}$ (Hz)[c]	$^{1}D_{CH}$ (Hz)[d]	$^{1}D_{CH}$ N^d (Hz)[e]
Gal1	162.33	162.80	173.81	11.48	11.01
Gal2	152.03	151.80	158.82	6.79	7.02
Gal3	147.48	148.59	156.82	9.34	8.23
Gal4	146.45	146.28	116.03	-30.42	-30.25
Gal5	142.08	142.24	153.76	11.68	11.52
Gal6	144.47	144.50	137.25	-7.22	-7.25
Glc1β	161.85	161.85	156.33	-5.52	-5.52
Glc2β	144.66	144.95	142.75	-1.91	-2.20
Glc3β	145.14	145.01	143.57	-1.57	-1.44
Glc4β	147.90	148.39	140.23	-7.67	-8.16
Glc5β	143.48	143.40	139.07	-4.41	-4.33
Glc6β	143.99	144.23	141.39	-2.6	-2.84
Glc1α	170.18	170.18	163.68	-6.5	-6.50
Glc2α	144.23	144.70	160.56	16.33	15.86
Glc3α	145.99	146.51	163.07	17.08	16.56
Glc4α	145.14	144.80	155.10	9.96	10.30
Glc5α	145.70	146.36	160.72	14.86	14.20
Glc6α	144.26	144.36	129.31	-14.95	-15.05
Gal1-2	7.80	7.92	12.36	4.56	-4.44
Glc1β-2β	7.96	8.14	3.78	-4.18	-4.36
Glc1α-2α	3.76	3.66	11.40	7.64	7.74

Also, J couplings can also be extracted from a J Scaled BIRD HSQC in the N^d phase sample conditions, just by raising the temperature up to a point where isotropic conditions are recovered. In those conditions, one noteworthy feature is that despite at that temperature DSCG is not forming a LC phase anymore, it is yet aggregated in such a way that peaks corresponding to DSCG are broad enough to be silent in the coupled HSQC experiments (see Supporting information). This would make possible the acquisition of both isotropic and anisotropic experiments using the same sample, since a change in temperature in 4K degrees (the lower limit for the LC phase in the N^d experimental conditions is 298K and completely isotropic conditions are obtained at 302K), would allow to turn back and forth into each of the phases. Also, as can be seen in **Table 1**, $^{1}J_{CH}$ coupling values extracted in isotropic conditions at 303K when DSCG is present in the sample are not significantly different with respect to the ones obtained in D_2O. This would be especially useful in cases where small amounts of sample are available, allowing to turn back and forth into each of the desired conditions in the same sample just by performing minor changes in the temperature.

5-Norbornen-2-ol

A slightly apolar and rigid spherically-shaped molecule like 5-norbornen-2-ol **Fig. 2.3** with both endo and exo isomers present in solution was used to expand the range of applicability of the DSCG medium and also to test the quality of RDC data in order to discriminate between both isomers. Signals were assigned to each isomer based on the relative value of their integrals, allowing the calculation of their relative proportions in the sample, which was unknown and resulted being 75:25 in favour of the endo isomer. Since the ^{13}C spectrum of the sample shows signal overlapping J Scaled F1 coupled BIRD HSQC was used again.

A total of 14 RDCs were measured and they were then split into two separate RDC input files depending on the value of the integrals found for each peak in the 1D ^{1}H experiment. Each data set was fit to the DFT optimized model of each isomer. $^1D_{CH}$ methylene couplings were treated in the SVD fitting as previously described.[39] One of the isomers was clearly selected by each RDC data set (Q factors of 0.059 and 0.070 were obtained for the endo and exo isomers using the correct RDC data sets for each one, while 0.122 and 0.135 were obtained using the wrong ones). Until now the results indicate the suitability of DSCG for the study of non-ionic molecules in water.

N-Methyl-codeinium iodide

Finally, we tested the compatibility of the DSCG phases with ammonium salts. The possibility of being able to study salts of organic compounds is a really interesting feature, since many pharmacologically active compounds are present in the form of salts. The alkaloid derivative N-methyl-codeinium iodide **Fig. 2.4** was studied in a 9 wt% N^d phase. This increment in the amount of DSCG used to form the LC phase was motivated by the stabilizing effect of ammonium salts on the DSCG isotropic phase.

For *N*-methyl-codeinium iodide the *J* Scaled F1 coupled HSQC spectrum is very well spread out and both the assignment of the signals and the data extraction was very straightforward. Signal to noise ratios between 12-30 were found in the coupled HSQC experiment (S/N intensities were calculated using the SNR peak calculator implemented in MestreNova 8.0.2). The RDC data set was fitted to the correct stereoisomer of *N*-methyl-codeinium iodide DFT optimized structure, taken from previous work.[19] A good quality factor was obtained (0.097) with a SVD condition number of 7.6. Attempts to study the brucine hydrochloride salt were unsuccessful to this point, since adding usual amounts of sample in the chromonic phase made the phase precipitate. Hence DSCG LC phases can be in principle also used with ionic compounds although phase stability problems may appear.

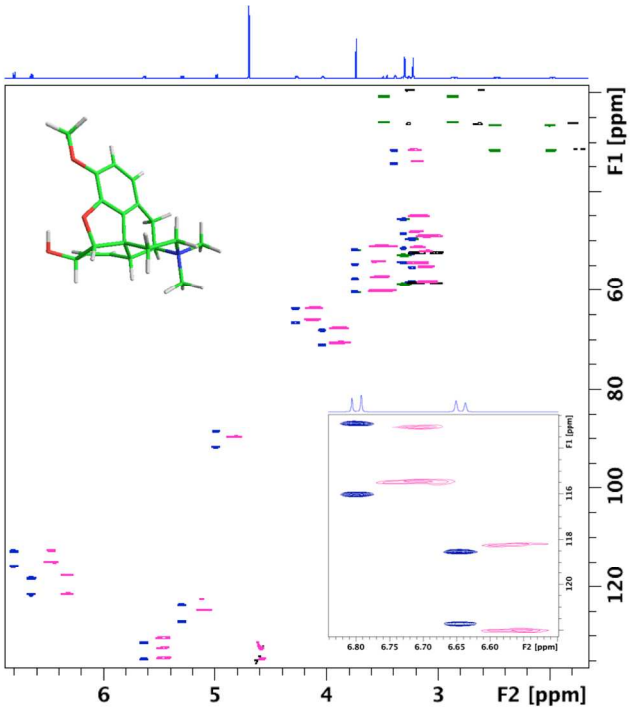

Fig. 9 Superimposed *J*-Scaled BIRD HSQC *N*-methyl-codeinium iodide isotropic experiment in D_2O (blue: positive contours, green: negative) and anisotropic experiment in the N^d phase (pink: positive, black: negative), with the aromatic signals amplified.

Conclusions

Disodium cromoglycate nematic LC phase has been demonstrated to be a good weakly aligning media for small water-soluble organic molecules. The medium is compatible with a variety of samples regarding their polarity, and the degree of alignment can be tuned by varying the mesogen concentration, the temperature and by addition of brine. This last feature was the most interesting one, since it reduces the degree of alignment of the LC phase, and yields RDC absolute values in a more manageable range. At the same time, small variation of the temperature allows to measure anisotropic and isotropic experiments in the same sample, with no losses in spectral resolution, no interferences of the mesogen signals and without significant changes in the values of the scalar couplings when compared to the experiment in D_2O.

Experimental

Materials and methods

Cromolyn disodium salt hydrate ($C_{23}H_{14}Na_2O_{11}\cdot H_2O$; MW=512.33 Da as anhydrous) was purchased from TCI Europe (purity >98.0%); 5-norbornen-2-ol ($C_7H_{10}O$; MW=110.15 Da) was purchased from Sigma Aldrich (purity 99%) as a mixture of the *–endo* and *–exo* isomers; methyl-β-D-galactopyranoside ($C_7H_{14}O_6$; MW=194.18 Da) was purchased from Sigma Aldrich; D-(+)-lactose monohydrate ($C_{12}H_{22}O_{11}\cdot H_2O$; MW=343.20 Da as anhydrous) was purchased from Sigma Aldrich; *N*-methyl-codeinium iodide was synthesized following a literature procedure.[45] All reagents were used without further purification and amounts between 8 and 10 mg of each compound were used to perform all the NMR experiments.

NMR methodologies

^{1}H and ^{2}H cromolyn studies were performed on a Bruker AVANCE III spectrometer of 400.16 MHz for the frequency of ^{1}H, 101 MHz for ^{13}C, and 60.38 MHz for ^{2}H. Isotropic samples were shimmed with the TopShim routine present in TopSpin 2.1, while anisotropic samples were heated up to the point were isotropic conditions were recovered (^{2}H spectra were recorded to check that the deuterium signal no longer splits into a doublet), automatically shimmed using TopShim and then samples were allowed to cool down to the original temperatures.

Pseudo-2D ^{2}H experiments were collected on a Bruker AVANCE I spectrometer of 600.13 MHz for the frequency of ^{1}H, 150.90 MHz for ^{13}C, and 90.56 MHz for ^{2}H, and equipped with a TBI probe. An experiment that uses a selective excitation pulse in the presence of a gradient was used to record the spectra. A gradient strength of 55.5 G/cm was used, which corresponds to a spatial frequency gradient in the z-axis of 17974 Hz/cm. A Gaussian cascade selective excitation pulse Q5[46] (shape Q5.1000 from Bruker library) was used with a duration of 6180 µs, corresponding to an excitation bandwidth of 1000 Hz. At a frequency gradient of 17974 Hz/cm, this excitation bandwidth corresponds to a z-slice of 0.55 mm. A total of 31 spatially resolved 1D ^{2}H NMR experiments (one at the center and 15 above and below the center of the coil) were collected sweeping the offset frequency (SPOFFS) from -30000 to +30000 Hz with a phase alignment SPOAL = 1 in steps of 2000 Hz. The automation program popt from the Bruker library was used for this purpose, and the option "store as 2D data" was checked in order to generate the pseudo-2D datasets. Spectra were acquired with 2 scans per slice and experiments were processed in magnitude and baseline correction was applied in the F2 dimension.

^{1}H, ^{13}C, COSY and HSQC needed to assign the signals of each compound and ^{13}C gated-decoupled experiments performed on methyl-β-D-galactopyranoside were performed on a Bruker AVANCE III spectrometer of 400.16 MHz for the frequency of ^{1}H, 101 MHz for ^{13}C, and 60.38 MHz for ^{2}H. *J* Scaled F1 Coupled HSQC and P.E.COSY experiments were performed on a Bruker AVANCE I spectrometer of 600.13 MHz for the frequency of ^{1}H, 150.90 MHz for ^{13}C, and 90.56 MHz for ^{2}H. ^{13}C gated-decoupled experiments were acquired using the zggd pulse sequence of the Bruker catalogue using 64k points (32k complex points) and a relaxation delay d1 of 0.1 s. Spectral window was centered between 20 and 120 ppm (sw=100 ppm, o1p=70 ppm). The respective experiments in the different LC phases were acquired using 8k scans and they were apodized with an exponential window function of 1.00. F2-coupled methyl-β-D-galactopyranoside experiments in the N and Nd phases were acquired at 293K with 16 scans, 2048 points in F2 and 256 in F1 and spectral windows of 1.8 ppm in the direct dimension and 60 ppm in the indirect one, setting the offset in the indirect dimension at 80 ppm. Lactose *J* Scaled BIRD HSQC experiments in isotropic (D_2O) and anisotropic conditions (cromolyn/NaCl) were acquired at 293K with 12 scans, 640 points in F2 and 2048 in F1 and spectral windows of 6 ppm in the direct dimension and 60 ppm in the indirect dimension, setting the offset in the indirect dimension at 82.5 ppm. In the case of the *J* Scaled BIRD HSQC at 303K in isotropic conditions in the sample with cromolyn/NaCl, 4 scans were acquired with 1024 points in F2 and 2048 points in F1, and spectral windows of 10 ppm and 100 ppm in F2 and F1 respectively, in order to check if signals from cromolyn would appear in the aromatic region of the spectrum. Lactose p.e.COSY experiment in anisotropic conditions was acquired at 293K with 4 scans, 4096 points in F2 and 1024 in F1 and spectral windows of 1.5 ppm in both dimensions. 5-Norbornen-2-ol *J* Scaled BIRD HSQC experiments were acquired at 293K with 24 scans, 896 points in F2 and 2048 in F1 and spectral windows of 8 ppm in the direct dimension and 160 ppm in the indirect dimension, setting the offset in the indirect dimension in 80 ppm. *N*-methyl-codeinium iodide *J* Scaled BIRD HSQC experiments were acquired at 293K with 4 scans for the isotropic sample and 8 for the anisotropic one, 512 points in F2 and 2048 in F1 and spectral windows of 6 ppm in the direct dimension for the isotropic sample and 5.5 for the anisotropic sample, and 160 ppm in the indirect dimension, setting the offset in the indirect dimension in 80 ppm. All *J* Scaled BIRD HSQC were performed using a scaling factor κ=3 for the C-H coupling. An HETCOR experiment was used to try to obtain isotropic and anisotropic peaks from *N*-methyl codeinium iodide in the same experiment at 299K. The experiment was acquired with 65K points in F2 and 128 in F1, with spectral windows of 140.0 and 10.0 ppm in F2 and F1 respectively.

Computational methodologies

A D-(+)-lactose molecular dynamics run was provided by Martín-Pastor from a previous study on lactose.[44] The structures from the MD run were optimized at DFT level using the B3LYP[47] functional and the 6-311G* basis set using Gaussian09.[48] We include here only the geometry for the RDC best fit structure, which corresponds to the syn-syn conformation. 5-Norbornen-2-ol 3D structures were generated with OpenBabel-2.3.1[49,50] from 2D ChemDraw structures, and they were DFT optimized using B3LYP/6-311G* as functional and basis set combination. The *N*-methyl-codeinium iodide structure that rendered the best *Q* factor in a previous work in our group[51] was used as a model to fit the RDC data extracted for it. The structures rendered by a MMFF94s[52,53] molecular mechanics (MM) conformational search were then DFT optimized using M06L[54] functional and the 6-31G** basis set. The lowest energy structure named as MCI_1A was the one used to fit the RDC data extracted from the cromolyn/NaCl medium. All calculations were performed using water IEFPCM as solvent model.[55]

Acknowledgements

We thank Gobierno de España for financial support (CTQ2011- 28831). A.N.V. thanks Spanish government for a Ramón y Cajal research contract. We thank Centro de Supercomputación de Galicia (CESGA) for computing time. We thank Dr. Manuel Martín Pastor for the Molecular Dynamics data of D-(+)-lactose.

Notes and references

[a] *Departamento de Química Orgánica, Edificio de Ciencias Experimentais, Campus Lagoas-Marcosende, Vigo, 36310 Spain. E-mail: armando.navarro@uvigo.es; mcid@uvigo.es; Fax: +34986812262; Tel: +34986813563*

† Electronic Supplementary Information (ESI) available: [details of any supplementary information available should be included here]. See DOI: 10.1039/b000000x/

1 C.M. Thiele, *Concepts in Mag. Reson*., 2007, **30**, 65–80.
2 G. Kummerlöwe, B. Luy, *TrAC Trends Anal. Chem.*, 2009, **28**, 483–493.
3 P. Trigo-Mourino, A. Navarro-Vázquez, J. Ying, R.R. Gil, A. Bax, *Angew. Chem. Int. Ed.,* 2011, **50**, 7576–7580.
4 A. Enthart, J.C. Freudenberger, J. Furrer, H. Kessler, B. Luy, *J. Magn. Reson.*, 2008, **192**, 314–322.
5 K. Fehér, S. Berger, K.E. Kövér, *J. Magn. Reson.*, 2003, **163**, 340–346.
6 P. Tzvetkova, S. Simova, B. Luy, *J. Magn. Reson.*, 2007, **186**, 193–200.
7 A. Navarro-Vázquez, *Magn. Reson. Chem.*, 2012, **50**, S73–S79.
8 A. Schuetz, J. Junker, A. Leonov, O.F. Lange, T.F. Molinski, C. Griesinger, *J. Am. Chem. Soc.*, 2007, **129**, 15114–15115.
9 H. Sun, U.M. Reinscheid, E.L. Whitson, E.J. d'Auvergne, C.M. Ireland, A. Navarro-Vázquez, C. Griesinger, *J. Am. Chem. Soc.*, 2011, **133**, 14629–14636.
10 V. Madiot, D. Gree, R. Gree, P. Lesot, J. Courtieu, *Chem. Commun*., 2000, 169–170.
11 C.M. Thiele, S. Berger, *Org. Lett*., 2003, **5**, 705–708.
12 M.D. Poliks, Y.W. Park, E.T. Samulski, *Mol. Cryst. Liq. Cryst*., 1987, **153**, 321–346.
13 V.V. Klochkov, B.I. Khairutdinov, A.V. Klochkov, M.S. Tagirov, C.M. Thiele, S. Berger, I.S. Vershinina, I.I. Stoikov, I.S. Antipin, A.I. Konovalov, *Russ. Chem. Bull. Int. Ed.*, 2004, **53**, 1–5.
14 C. Gayathri, N.V. Tsarevsky, and R.R. Gil, *Chem. Eur. J.*, 2010, **16**, 3622–3626.
15 G. Kummerlöwe, J. Auernheimer, A. Lendlein, B. Luy, *J. Am. Chem. Soc.,* 2007*,* **129**, 6080-6081.
16 J.C. Freudenberger, P. Spiteller, R. Bauer, H. Kessler, B. Luy, *J. Am. Chem. Soc.,* 2004, **126**, 14690-14691.
17 K. Kobzar, H. Kessler, B. Luy, *Angew. Chem. Int. Ed.,* 2005, **44**, 3145 –3147.
18 C. Merle, G. Kummerlöwe, J.C. Freudenberger, F. Halbach, W. Stöwer, C.L. V Gostomski, J. Höpfner, T. Beskers, M. Wilhelm, B. Luy, *Angew. Chem. Int. Ed.*, 2013, **52**, 10309–10312.
19 P. Haberz, J. Farjon, C. Griesinger, *Angew. Chem. Int. Ed.,* **2005**, *44*, 427–429.
20 J. Lydon, *J. Mater. Chem*., 2010, **20**, 10071–10099.
21 J. Lydon, *Curr. Opin. Colloid Interface Sci.*, 2004, **8**, 480–490.
22 S.W. Tam-Chang, L. Huang, *Chem. Commun.*, 2008, 1957–1967.
23 S. Vasilevskaya, E.V. Generalova, A.S. Sonin, *Russ. Chem. Rev.*, 1989, **58**, 904–916.
24 O.D. Lavrentovich, M. Sergan, J. Kelly, *Liq. Cryst*., 2003, **30**, 851–859.
25 S.V. Shiyanovskii, O.D. Lavrentovich, T. Schneider, T. Ishikawa, I.I. Smalyukh, C.J. Woolverton, G.D. Niehaus, K.J. Doane, *Mol. Cryst. Liq. Cryst*., 2005, **434**, 587–598.
26 S.V. Shiyanovskii, T. Schneider, I.I. Smalyukh, T. Ishikawa, G.D. Niehaus, K.J. Doane, C.J. Woolverton, O.D. Lavrentovich, *Phys. Rev. E*, 2005, **71**, 020702(1)–020702(4).
27 C.J. Woolverton, E. Gustely, L. Li, O.D. Lavrentovich, *Liq. Cryst*., 2005, **32**, 417–423.
28 M.V. Paukshto, E-type polarizers and their applications, Optiva Inc, San Fransisco, 2001, 89.
29 F. Chami, M.R. Wilson, *J. Am. Chem. Soc.*, 2010, **132**, 7794–7802.
30 L.J. Yu, A. Saupe, *Mol. Cryst. Liq. Cryst*., 1982, **80**, 129–134.
31 J.M. Péchiné, A. Meddour, J. Courtieu, *Chem. Commun*., 2002, 1734–1735.
32 A.F. Kostko, B.H. Cipriano, O.A. Pinchuk, L. Ziserman, M.A. Anisimov, D. Danino, S.R. Raghavan, *J. Phys. Chem. B*, 2005, **109**, 19126–19133.
33 P. Trigo-Mouriño, C. Merle, M.R.M. Koos, B. Luy, R.R. Gil, *Chem. Eur. J.*, 2013, **19**, 7013–7019.
34 J.S.G. Cox, G.D. Woodard, W.C. McCrone, *J. Pharm*. Sci., 1971, **60**, 1458–1465.
35 N.H. Hartshorne, G.D. Woodard, *Mol. Cryst. Liq. Cryst*., 1973, **23**, 343–368.
36 C.M. Thiele, W. Bermel, *J. Magn. Reson.*, 2012, **216**, 134–143.
37 J. Furrer, M. John, H. Kessler, B. Luy, *J. Biomol. NMR*, 2007, **37**, 231–243.
38 J.R. Tolman, J.H. Prestegard, *J. Magn. Reson. B*, 1996, **112**, 269–274.
[39] P. Trigo-Mouriño, R. Santamaría-Fernández, V.M. Sánchez-Pedregal, A. Navarro-Vázquez, *J. Org. Chem.*, 2010, **75**, 3101–3114.
40 J.D. Snider, E. Troche-Pesqueira, S.R. Woodruff, C. Gayathri,, V. Tsarevsky, R.R. Gil, *Magn. Reson. Chem.*, 2012, **50**, S86-S91.
41 L. Mueller, *J. Magn. Reson*., 1987, **196**, 191–196.
42 G. Cornilescu, J.L. Marquardt, M. Ottiger, A. Bax, *J. Am. Chem. Soc.*, 1998, **120**, 6836-6837.
43 J.A. Losonczi, M. Andrec, M.W.F. Fischer, J.H. Prestegard, *J. Magn. Reson.*, 1999, **138**, 334-342.
44 M. Martín-Pastor, A. Canales, F. Corzana, J.L. Asensio, J. Jiménez-Barbero, *J. Am. Chem. Soc.*, 2005, **127**, 3589–3595.
45 R. W. Seidel, B. R. Bakalska, T. Kolev, D. Vassilev, H. Mayer-Figge, M. Spiteller, W. S. Sheldrick, B. B. Koleva, *Spectrochim. Acta, Part A*, 2009, **73**, 61.
46 L. Emsley, G. Bodenhausen, *J. Magn. Reson*., 1992*,* **97***, 135*.
47 A. D. Becke, J. *Chem. Phys*., 1993,**98**, 5648.
48 M. J. Frisch, G. W. Trucks, H. B. Schlegel, G. E. Scuseria, M. A. Robb, J. R. Cheeseman, G. Scalmani, V. Barone, B. Mennucci, G. A. Petersson, H. Nakatsuji, M. Caricato, X. Li, H. P. Hratchian, A. F. Izmaylov, J. Bloino, G. Zheng, J. L. Sonnenberg, M. Hada, M. Ehara, K. Toyota, R. Fukuda, J. Hasegawa, M. Ishida, T. Nakajima, Y. Honda, O. Kitao, H. Nakai, T. Vreven, J. A. Montgomery Jr., J. E. Peralta, F. Ogliaro, M. Bearpark, J. J. Heyd, E. Brothers, K. N. Kudin, V. N. Staroverov, R. Kobayashi, J. Normand, K. Raghavachari, A. Rendell, J. C. Burant, S. S. Iyengar, J. Tomasi, M. Cossi, N. Rega, J. M. Millam,M. Klene, J. E. Knox, J. B. Cross, V. Bakken, C. Adamo, J. Jaramillo, R. Gomperts, R. E. Stratmann, O. Yazyev, A. J. Austin, R. Cammi, C. Pomelli, J. W. Ochterski, R. L. Martin, K.Morokuma, V. G. Zakrzewski, G. A. Voth, P. Salvador, J. J. Dannenberg, S. Dapprich, A. D. Daniels, Ö. Farkas, J. B. Foresman, J. V. Ortiz, J. Cioslowski, D. J. Fox, R. A. Gaussian 09, Gaussian, Inc,Wallingford CT, **2009**.
49 N. M. O'Boyle, M. Banck, C. A. James, C. Morley, T. Vandermeersch and G. R. Hutchison, *J. Cheminf*., 2011, **3**, 33.
50 The Open Babel Package, version 2.3.1, http://openbabel.org.
51 P. Trigo-Mouriño, A. Navarro-Vázquez, and V. M. Sánchez-Pedregal, *Magn. Reson. Chem.*, 2012, **50,** S29–S37.
52 T. A. Halgren. *J. Comp. Chem*. 1996, **17**, 490–519.
53 T. A. Halgren. *J. Comp. Chem*. 1999, **20**, 730–748.
54 Y. Zhao and D. G. Truhlar, *J. Chem. Phys*., 2006, **125**, 194101.
55 J. Tomasi, B. Mennucci and R. Cammi, *Chem. Rev*., 2005, **105**, 2999.